



Kinetic study of the pyrolysis of miscanthus and its acid hydrolysis residue by thermogravimetric analysis



Ana María Cortés, A.V. Bridgwater *

Bioenergy Research Group, European Bioenergy Research Institute, Aston University, Birmingham B4 7ET, UK

ARTICLE INFO

Article history:

Received 5 February 2015

Received in revised form 18 May 2015

Accepted 19 May 2015

Available online xxx

Keywords:

Kinetics

Acid hydrolysis residue

Thermogravimetric analysis

Activation energy

Pre-exponential factor

Isoconversional methods

ABSTRACT

The kinetic parameters of the pyrolysis of miscanthus and its acid hydrolysis residue (AHR) were determined using thermogravimetric analysis (TGA). The AHR was produced at the University of Limerick by treating miscanthus with 5 wt.% sulphuric acid at 175 °C as representative of a lignocellulosic acid hydrolysis product. For the TGA experiments, 3 to 6 g of sample, milled and sieved to a particle size below 250 µm, were placed in the TGA ceramic crucible. The experiments were carried out under non-isothermal conditions heating the samples from 50 to 900 °C at heating rates of 2.5, 5, 10, 17 and 25 °C/min. The activation energy (E_A) of the decomposition process was determined from the TGA data by differential analysis (Friedman) and three isoconversional methods of integral analysis (Kissinger–Akahira–Sunose, Ozawa–Flynn–Wall, Vyazovkin). The activation energy ranged from 129 to 156 kJ/mol for miscanthus and from 200 to 376 kJ/mol for AHR increasing with increasing conversion. The reaction model was selected using the non-linear least squares method and the pre-exponential factor was calculated from the Arrhenius approximation. The results showed that the best fitting reaction model was the third order reaction for both feedstocks. The pre-exponential factor was in the range of 5.6×10^{10} to $3.9 \times 10^{13} \text{ min}^{-1}$ for miscanthus and 2.1×10^{16} to $7.7 \times 10^{25} \text{ min}^{-1}$ for AHR.

© 2015 Published by Elsevier B.V.

1. Introduction

The growing worldwide concern over fossil fuel resource depletion and greenhouse gas emissions from their utilisation has intensified the search for new and renewable energy sources. The role of lignocellulosic biomass has become significant among the multiple reusable natural resources, as gas and liquid fuels and chemicals can be directly obtained without adding new carbon dioxide to the atmosphere [1]. Biomass from either energy crops or agricultural residues can be thermally and/or chemically treated under different conditions to obtain liquids or gases according to the desired application. Two feed materials have been studied: miscanthus and the acid hydrolysis residue of miscanthus processing. Chemical transformation of lignocellulosic biomass into platform chemicals such as hydroxymethyl furfural, furfural and levulinic acid for production of chemicals and/or diesel miscible biofuels can be achieved by hydrolysis. The process is typically carried out at temperatures between 100 and 250 °C in the presence of an acid catalyst and is known as acid hydrolysis [2]. The non-reactive product of acid hydrolysis contains insoluble lignins and intractable cellulose condensation products known as humins which together are referred to as acid hydrolysis residue (AHR) [2]. This is the feed material used in this study to evaluate potential uses for this waste stream. AHR is a black powder that can be separated by filtration, containing up to 80% of the

energy of the original feedstock. The first report on the use of AHRs to produce energy or biofuels known to the authors is the work from Girisuta et al. [3]. Catalytic pyrolysis was used to transform AHRs from miscanthus obtained at different hydrolysis conditions into bio-oil [3]. In later studies, Hoang et al. investigated the catalytic gasification of humins to produce hydrogen [4] and syngas [5].

Within energy crops, *Miscanthus × giganteus* is regarded as a feedstock with high potential for thermochemical processes due to its particular characteristics, such as high C:N ratio and high energy production per hectare of up to 20 dry t/ha in northern climates [6]. Due to these properties and its high cellulose content (27–50 wt.% dry basis) it has been used for acid hydrolysis for production of chemicals such as hydroxymethyl furfural, furfural and levulinic acid. These are valuable both as chemicals and as fuel additives. This work focuses on miscanthus and the solid residue from acid hydrolysis of miscanthus and includes a comparison of these two materials. Although the AHR is relatively unreactive, it is essential to realise its energy content either through combustion for heat production and hence power generation or through gasification either for power generation or biofuel production. The increasing interest in production of platform chemicals from biomass means that processes such as acid hydrolysis will become increasingly common and widely used, so viable uses for the residues are essential to optimise such processes.

Miscanthus is a C4 perennial grass and has a higher lignin content compared to woody biomass [6]. Lignin is one of the main constituents of biomass (18 to 25 wt.% dry basis) and, after cellulose; is the second

* Corresponding author.

most abundant polymer in nature. The carbon content in lignin is around 60% [7,8]. During the acid hydrolysis transformation, lignin and other cellulose condensation reaction products (humins) form a solid residue often referred to as acid hydrolysis residue (AHR). Up to 80% of the energy of the feedstock is stored in the AHR, which can potentially be recovered by thermal processing [3]. One interesting process that could be used to recover either energy (via the production of liquid oil) or valuable chemicals from the AHR is pyrolysis. Pyrolysis is defined as the treatment of solid fuels in the absence of oxygen at moderate temperatures (450 to 550 °C) [9]. The yield of the liquid product can be maximised up to 75 wt.% by means of high heating rates, low hot vapour residence time and rapid quenching of the vapours to minimize secondary reactions. A kinetic description of the pyrolysis process is necessary for design, modelling and optimization of large scale applications. Determining the reaction models and kinetic parameters for each individual reaction requires a complex series of experimental, analytical and mathematical stages. However, the apparent kinetics of the thermal decomposition considered as a single step are a good approximation to describe and compare different feedstocks [10–13].

1.1. TGA kinetics

Thermogravimetric analysis (TGA) is a rapid, precise technique to determine the mass loss of a sample over time and evaluate the thermal decomposition of solids and its kinetics [14]. An initial investigation of the pyrolysis behaviour can be performed by TGA, however, the method has been criticized as limited for kinetics determination, as it only allows the analysis to be performed at relatively slow heating rates. These results are often extrapolated to fast pyrolysis heating rates which are considerably higher, leading to inaccurate and potentially misleading results [11]. Nevertheless, different samples can be easily and rapidly compared with TGA, and it is possible to determine basic parameters for slow pyrolysis modelling [11,12,14].

Kinetic parameters can be calculated using two different experimental TGA methods. In the isothermal method, decomposition measurements are performed at constant temperature [12,15]. The alternative is the dynamic or non-isothermal method which is usually preferred as the full temperature range is considered. The sensitivity and error can be improved if the measurements are performed using different linear heating rates and the kinetic parameters can be calculated using isoconversional methods [12,16]. Different mathematical and analytical approximations can be used to calculate the kinetic parameters by from the temperature integral [17]. The approximations developed by Friedman, Ozawa–Flynn–Wall (OFW), Kissinger–Akahira–Sunose (KAS) and Vyazovkin are among the most commonly used [11,17]. A non-isothermal, isoconversional approach was used in the present work to determine the kinetic parameters of the pyrolytic decomposition of miscanthus and its AHR and the results obtained by the different approximations mentioned were compared.

To the knowledge of the authors, no comparison between all these methods has been performed for biomass pyrolysis. Some studies have compared results obtained by two of them. Yang and Wu compared the values of kinetic parameters for pyrolysis of wheat straw's enzymatic acidolysis lignin obtained using the OFW and KAS approximations [13]. TGA measurements were performed using 6 to 12 mg of sample at maximum temperature of 800 °C reached at heating rates of 10, 20, 30, 40 and 50 °C/min using nitrogen. Only one value for each parameter was reported in the study. Using the OFW method, the activation energy and the pre-exponential factor were 107.69 kJ/mol and 20.60 min⁻¹, respectively. The values calculated by the KAS method were slightly lower, 103.92 kJ/mol for the activation energy and lnk₀ = 19.2 min⁻¹.

Hilten et al. compared the kinetic parameters obtained by the Friedman and the KAS methods for pyrolysis of Sorghum bicolor. The kinetic calculations were performed using only the data corresponding to conversions between 5 and 60 wt.% due to the inconsistency of data above 60%. The average activation energy for stem and leaf samples

was 229.7 kJ/mol with a standard deviation of 40 when the Friedman method was used. No considerable difference was found when using the KAS method, for which the average value for stems and leaves was 223.6 kJ/mol with standard deviation 35.5 kJ/mol.

Ounas et al. compared the results obtained by the Vyazovkin and OFW methods for pyrolysis kinetics of olive residue and sugarcane bagasse [18]. The authors reported that similar activation energy values were obtained by both methods, with slightly higher values when calculated by the Vyazovkin method. A summary of all results is presented in Table 1 to compare the results obtained by different calculation methods. The authors did not report values for lignin but values reported by other authors are included in Tables 4 and 5 for comparison with values obtained for AHR in this work.

A comparison between the kinetic parameters calculated using the KAS and OFW methods has been made for TGA pyrolysis of cardoon [19]. The activation energy using both methods was very similar for stems but slightly lower for leaves when calculated by KAS (230 kJ/mol stems and 242 kJ/mol for leaves). The value for pre-exponential factor was also slightly lower when calculated by KAS (4.3–6.5E + 17 for stems and 6.5–9.5E + 28 for leaves), while the reaction order was in the same range for both fractions (n = 8–9 for stems and n = 14–15 for leaves).

2. Materials and methods

2.1. Preparation of samples

Miscanthus × giganteus was supplied by the University of Limerick in the Republic of Ireland from a local source and received as shown in Fig. 1. *Miscanthus* was collected in April 2012 from the Limerick County area and was milled in an industrial Retsch SM200 cutting mill using a 4 mm reference sieve. The particle size was further reduced in the same system using a 1 mm sieve. The feedstock was then ground using a kitchen coffee grinder and sieved to separate the fraction with a particle size below 250 µm.

The AHR was produced at the University of Limerick by treating miscanthus with 5 wt.% sulphuric acid at 175 °C for 1 h, following the procedure described elsewhere [3]. In the acid hydrolysis process, biomass was fed into the reactor with water in a 1:9 solid to liquid ratio and then the mixture was heated to 175 °C. Sulphuric acid was added after equalizing the pressure to that inside the reactor. After the reaction time was reached, the mixture was separated by filtration and the solid residue was washed with water several times and oven-dried overnight at 60 °C. When received, the residue was sieved and the fraction with particles below 250 µm (more than 85 wt.% of the original sample) was used for the TGA measurements.

2.2. Proximate and ultimate analysis

Elemental (C, H, N) analysis was carried out externally by Medac Laboratories Ltd using a Carlo-Erba EA1108 analyser. The oxygen content was calculated by difference from the results received from the laboratory. Moisture, char and volatiles were determined according to ASTM E1131 [20] using a PerkinElmer Pyris 1 TGA, heating the sample

Table 1
Results reported by Ounas et al. [18] for pyrolysis activation energy calculated by OFW and Vyazovkin methods.

Feedstock	Decomposition stage	E _A (kJ/mol)	
		Calculated by OFW	Calculated by Vyazovkin
Olive residue	Hemicellulose	148–158	158–166
	Cellulose	198–211	210–219
Sugarcane bagasse	Hemicellulose	163–173	176–184
	Cellulose	227–235	236–244



Fig. 1. As received miscanthus (left) and AHR from miscanthus (right).

to 900 °C at a rate of 10 °C/min and holding the temperature for 10 min to ensure constant final weight. Ash contents were determined using the TGA under nitrogen atmosphere by heating to 500 °C at a rate of c and holding for 10 min; then heating the residue under an air atmosphere to 575 °C at a rate of 2.5 °C/min and holding for 10 min. The ash contents of the raw feedstocks were also measured by ASTM E1755 [21]. The higher heating value (HHV) of the feedstocks was calculated using the equation proposed by Channiwala (Eq. (1)) [22].

$$\text{HHV} = 0.3491 \times C + 1.1783 \times H + 0.1005 \times S - 0.1034 \times O - 0.0151 \times N - 0.0211 \times \text{Ash} \quad (1)$$

2.3. Composition analysis

The separation of the structural carbohydrates cellulose, hemicellulose and lignin in miscanthus was performed by the wet chemistry method according to the small scale separation method proposed by Ona et al. [23]. A dry sample 3 to 6 g was used to determine the composition of each sample. Extractive free samples were prepared in a Soxhlet apparatus by treating the sample with toluene/ethanol, ethanol and water. The content of extractives was determined by weight difference after drying the extractives-free sample. The lignin content was determined by treating the extractives-free sample with concentrated (72 wt.%) and diluted (3 wt.%) sulphuric acid. The holocellulose fraction was separated by extracting the lignin with sodium acetate and chlorite. After delignification, hemicellulose was dissolved in 17.5 wt.% sodium hydroxide to separate the cellulose fraction. Residual lignin in hemicellulose was also diluted using concentrated and diluted sulphuric acid. The content of hemicellulose was calculated by subtracting between the weight of cellulose and residual lignin from the amount of holocellulose. Extractives and Klason lignin for the AHR were determined by the University of Limerick using the TAPPI method and reported elsewhere [3].

2.4. Thermogravimetric analysis

Thermogravimetric non-isothermal measurements were made according to the ASTM E1641-07 [24] method using a PerkinElmer Pyris 1 TGA. 3 to 6 mg of sample was placed in a tared ceramic crucible. Each sample was heated from 50 to 900 °C at heating rates of 2.5, 5, 10, 17.5 and 25 °C/min under a nitrogen flow of 20 ml/min. The final temperature was held for 10 min to ensure constant final weights.

3. Kinetic parameters estimation

The isoconversional methods developed by Friedman, Ozawa–Flynn–Wall, Kissinger–Akahira–Sunose and Vyazovkin were used to calculate the activation energy for each feedstock. The values obtained by the four methods were compared. Since there was no significant difference between the values obtained by the four methods and the

Vyazovkin method presents mathematical advantages (presented in Section 3.4); the values determined by this method were used to find the best fit among the reaction models described by different authors [12,14,25] and presented in Table 2. The best fitting model was determined using the non-linear least squares method and used for the calculation of the pre-exponential factor as described below.

The rate of decomposition of biomass can be formulated in terms of temperature (T) and conversion (α) [8,26]:

$$\frac{d\alpha}{dt} = k(T)f(\alpha). \quad (2)$$

The conversion can be expressed in terms of the mass fraction of biomass that has decomposed [12,16]:

$$\alpha = \frac{w_0 - w}{w_0 - w_f}. \quad (3)$$

The temperature dependent function is generally expressed by the Arrhenius equation in terms of the activation energy (E_A) and the pre-exponential factor (k_0) [8,26]:

$$k(T) = k_0 \exp\left(-\frac{E_A}{RT}\right). \quad (4)$$

Table 2
Conversion functions of reaction models used for the calculation of kinetic parameter using the Arrhenius equation [12,14,25].

Reaction model	$f(\alpha)$	$g(\alpha)$
Reaction order		
Order 0 (O0)	1	α
Order 1 (O1)	$(1-\alpha)$	$-\ln(1-\alpha)$
Order 2 (O2)	$(1-\alpha)^2$	$(1-\alpha)^{-1}$
Order 3 (O3)	$(1-\alpha)^3$	$\frac{1}{2}(1-\alpha)^{-2}$
Phase boundary controlled reaction		
Contracting area (R2)	$(1-\alpha)^{1/2}$	$1-(1-\alpha)^{1/2}$
Contracting volume (R3)	$(1-\alpha)^{2/3}$	$1-(1-\alpha)^{1/3}$
Diffusion		
1 dimension (D1)	$\frac{1}{2}\alpha$	α^2
2 dimensions (D2)	$[-\ln(1-\alpha)]^{-1}$	$(1-\alpha)\ln(1-\alpha) + \alpha$
3 dimensions by Jander (D3)	$\frac{3}{2}(1-\alpha)^{2/3}[1-(1-\alpha)^{1/3}]^{-1}$	$[1-(1-\alpha)^{1/3}]^2$
3 dimensions by Ginstling-Brounshei (D4)	$\frac{3}{2}[(1-\alpha)^{-1/3}-1]^{-1}$	$1-2\alpha/3-(1-\alpha)^{2/3}$
Nucleation		
Power law (P2, P3, P4 for $n = 2, 3, 4$)	$n\alpha^{(1-1/n)}$, $n = 2/3, 1, 2, 3, 4$	$\alpha^{1/n}$
Avrami–Erofeev (A1, A2, A3, A4 for $n = 1, 2, 3, 4$)	$n(1-\alpha)[- \ln(1-\alpha)]^{(1-1/n)}$ with $n = 1-4$	$[- \ln(1-\alpha)]^{1/n}$

The decomposition kinetic equation can be obtained combining these equations [8,26]:

$$\frac{d\alpha}{dt} = k_0 \exp\left(\frac{-E_A}{RT}\right) f(\alpha) \quad (5)$$

Under non-isothermal conditions, the actual temperature can be expressed in terms of the initial temperature (T_0) and the heating rate (β), allowing the calculation of the decomposition rate as function of temperature instead of time [26]:

$$T = T_0 + \beta t \quad (6)$$

$$\frac{d\alpha}{dT} = \frac{k_0}{\beta} \exp\left(\frac{-E_A}{RT}\right) f(\alpha). \quad (7)$$

The integral form of $f(\alpha)$ can be expressed as:

$$g(\alpha) = \int_0^\alpha \frac{d\alpha}{f(\alpha)} = \frac{k_0}{\beta} \int_0^{T_\alpha} \exp\left(\frac{-E_a}{RT}\right) dT. \quad (8)$$

Defining x as

$$x = \frac{E_A}{RT}. \quad (9)$$

The temperature integral can be expressed as a function of x :

$$g(\alpha) = \int_0^\alpha \frac{d\alpha}{f(\alpha)} = \frac{k_0 \cdot E_A}{\beta \cdot T} \int_x^\infty \frac{\exp(-x)}{x^2} dx = \frac{k_0 \cdot E_A}{\beta \cdot T} p(x) \quad (10)$$

where $p(x)$, referred to as the temperature integral, has no exact analytical solution and must be determined by means of empirical interpolations [26] like the ones used in the present work and described below.

3.1. Friedman method

The Friedman method is based on the assumption that the chemistry of the decomposition process depends only on the rate of mass loss and is independent from the temperature. Therefore, $f(\alpha)$ can be considered constant and taking natural logarithms at both sides of Eq. (7) gives the following equation [12,27]:

$$\ln \left[\beta \frac{d\alpha}{dT} \right] = \ln [k_0 f(\alpha)] - \frac{E_A}{RT}. \quad (11)$$

The activation energy can be calculated from the slope of the line obtained by plotting the left side of the equation against the inverse temperature.

3.2. Ozawa–Flynn–Wall method

The Ozawa–Flynn–Wall method (referred to as Ozawa in the present work) uses the Doyle linear approximation to calculate $p(x)$ for $20 \leq x \leq 60$ [12,28]:

$$\log p(x) = -2.315 - 0.4567 \cdot x \quad (12)$$

Replacing $p(x)$ in Eq. (10) and rearranging:

$$\log \beta = \log \left(\frac{k_0 \cdot E_A}{R \cdot g(\alpha)} \right) - 2.315 - 0.4567 \cdot \frac{E_A}{R \cdot T} \quad (13)$$

The values of E_A can be calculated from the slope of the plot of $\log \beta$ against the inverse temperature [12,28].

3.3. Kissinger–Akahira–Sunose method

Although it is normally used in model fitting methods, the Coats–Redfern temperature integral approximation can be modified to transform it for isoconversional calculations:

$$\ln \left[\frac{\beta}{T^2} \right] = \ln \left[\frac{k_0 R}{E_A g(\alpha)} \left(1 - \frac{2RT}{E_A} \right) \right] - \frac{E_A}{RT}. \quad (14)$$

The activation energy can be calculated from the plot of the logarithm of β/T^2 against the temperature inverse, taking into account that $2RT/E_A \ll 1$ for the temperature range considered. The Kissinger–Akahira–Sunose method (referred to as Kissinger in the present work) is based in this approximation using $p(x) = e^{-x}/x^2$ for $20 \leq x \leq 50$ [28,29].

3.4. Vyazovkin method

This method uses the nonlinear regression proposed by Senum and Yang, which makes it more accurate over a wider range of TGA data [11] and circumvents the inaccuracies related to the analytical approximation of the temperature integral. However, its application remains limited as mass transfer becomes limiting at conversions high conversions (above 80 wt.%) [30]. The temperature integral results from the ratio of two polynomials [30]:

$$p(x) \cong \frac{\exp(-x)}{x} \cdot \frac{x^3 + 18x^2 + 86x + 96}{x^4 + 20x^3 + 120x^2 + 240x + 120}. \quad (15)$$

Considering $p(x) = I(E_A, T_\alpha)$, the Vyazovkin method can be applied to calculate the activation energy value that minimizes $\Omega(E_A)$, a function of the activation energy for a set of temperature values calculated at the same conversion value α for n different heating rates [12,25,31]:

$$\Omega(E_A) = \sum_{j=1}^n \sum_{k \neq j}^n \frac{\beta_k I(E_A T_{\alpha j})}{\beta_j I(E_A T_{\alpha k})}. \quad (16)$$

In the present work, the $\Omega(E_A)$ function was minimized using the Solver function in Microsoft Excel.

3.5. Pre-exponential factor calculation by non-linear least squares method

Although the activation energy can be calculated with no knowledge of the $f(\alpha)$ or $g(\alpha)$ functions, the calculation of the pre-exponential factor requires the definition of the reaction model. The most common reaction models used to describe the behaviour of solid state reactions have been presented by different authors [12,14,31] and are summarised in Table 2. The selection of the reaction model is based on the minimization of the difference of the squares of the experimental $(d\alpha/dt)_{\text{exp}}$ and calculated $(d\alpha/dt)_{\text{calc}}$ DTG curves (differential thermogravimetric curves). The determination is based on the minimisation of the objective function $\Omega(E_A)$ in Eq. (17) [19,32].

$$\Omega(E_A) = \sum \left[\left(\frac{d\alpha}{dt} \right)_{\text{exp}} - \left(\frac{d\alpha}{dt} \right)_{\text{calc}} \right]^2 \quad (17)$$

where $(dm/dt)_{\text{exp}}$ is the experimentally observed DTG curve and $(dm/dt)_{\text{calc}}$ is the calculated DTG curve, obtained by numerical solution of the kinetic differential equation with the given set of parameters.

Table 3
Compositional, proximate and ultimate analysis for miscanthus and its acid hydrolysis residue (AHR).

	Miscanthus (this work)	Miscanthus (literature refs. [33,34])	AHR from miscanthus
Structural composition (wt.% on dry basis)			
Extractives	7.7	Not reported	6.9*
Klason lignin	21.9	10–25	91.2*
Cellulose	40.8	27–50	
Hemicellulose	29.6	20–35	
Elemental composition (wt.% on dry basis)			
Carbon	46.0	46–50	65.1
Hydrogen	6.0	5–6	4.5
Nitrogen	0.5	–0.5	0.4
Sulphur	No detectable	<0.1	0.2
Oxygen (by difference)	47.5	40–45	28.9
Moisture (wt.%)	5.7	4–12	3.5
Proximate analysis (wt.% on dry basis)			
Volatiles	72.9	65–70	42.7
Char	27.1	15–30	57.3
Fixed carbon	25.0	15–20	54.5
Ash	2.0	2–3	2.8
High heating value (kJ/g dry feedstock)	18.17	18–19	25.65
Low heating value (kJ/g dry feedstock)	16.99	Not reported	24.67

* Note: Structural composition values for AHR taken from [3].

4. Results and discussion

4.1. Feedstock characterisation

The proximate, ultimate and compositional analysis of miscanthus and its AHR were performed as described in Section 2.2 and the results are presented in Table 3. The difference in the lignin content of both feedstocks (21.9 wt.% for miscanthus and 91.2 wt.% for AHR) show how the acid hydrolysis process degrades the cellulose and hemicellulose fractions of the original feedstock into an amorphous polymer known as humins which is mixed with the residual lignin, with the mixed solid referred to as AHR. The humins are the product from condensation and polymerisation reactions between cellulose and

intermediate products of acid hydrolysis [3]; which are insoluble in concentrated sulphuric acid. Humins would be quantified as Klason lignin during the separation procedure, which only separates the sample into acid soluble and acid insoluble material. The effects of the degradation are reflected on the calculated residue heating value, which increases by more than 40% compared to miscanthus.

The low increase in ash content of the AHR compared to untreated miscanthus can be attributed to the demineralization effect of hot water and acid used in acid hydrolysis. Biomass pre-treatment using water and diluted acid (mainly hydrochloric) has been reported to reduce the alkali metal content in biomass [35–39] and has been used to improve the quality of bio-oil in fast pyrolysis studies [40]. The sulphur content in the AHR can be understood as residual sulphuric acid left

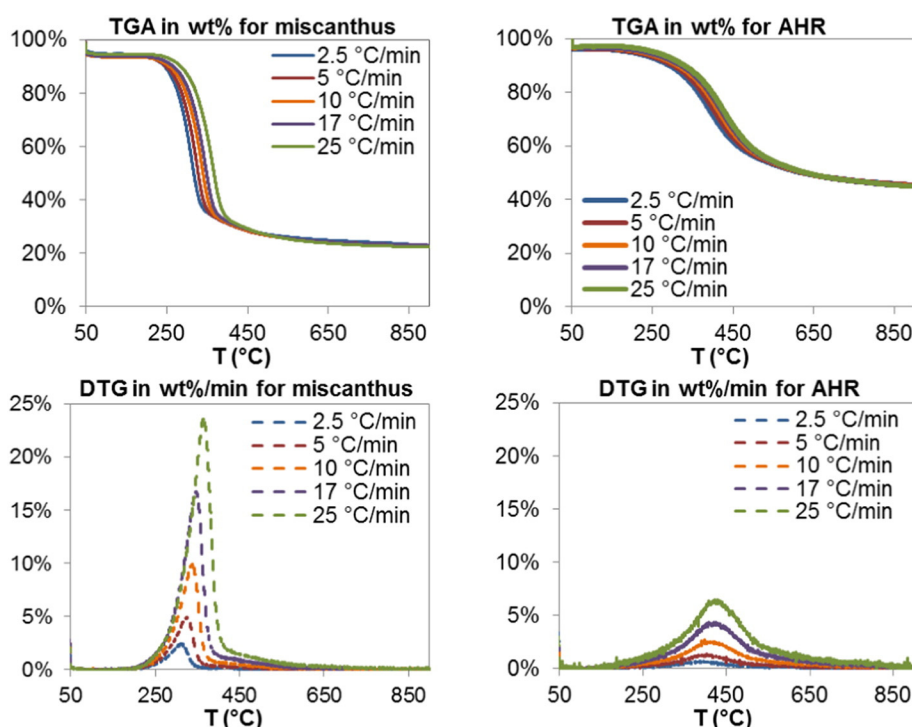


Fig. 2. TGA (continuous lines) and DTG (dashed lines) curves for miscanthus (left) and its AHR (right) at five different heating rates.

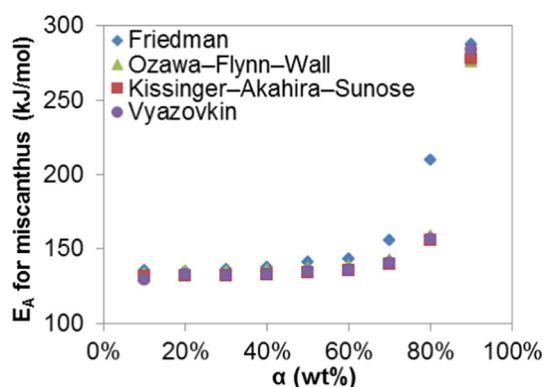


Fig. 3. Variation of the activation energy with conversion and calculation coefficients for pyrolysis of miscanthus by lineal (Friedman, Ozawa, Kissinger) and non-linear (Vyazovkin) methods.

after thoroughly washing the residue after the acid hydrolysis reaction (detailed processing presented elsewhere [3]), since the sulphur content of miscanthus was below detection levels.

4.2. Thermogravimetric analysis

Fig. 2 shows the TGA and DTG curves of miscanthus and its AHR at five different heating rates: 2.5, 5, 10, 17 and 25 °C/min. The decomposition curves under an inert atmosphere for both feedstocks present a single decomposition peak related to a primary pyrolysis stage. The peak is stronger for miscanthus due to the higher volatile content of this feedstock. For both feedstocks, a shift towards higher peak decomposition temperatures is observed with increasing heating rate. The same behaviour has been reported in the literature for miscanthus [41] and other biomass feedstocks such as demolition wood [42], sawdust [43], palm oil residues [42,44], pinewood [42], wood chips [26], olive residue, sugarcane bagasse [18], wheat straw enzymatic acidolysis lignin [13], cardoon [19], pine bark [45], corn and wheat straw [46], sorghum [47] and lignins [48]. The shifting of the decomposition curves is a result of heat and mass transfer limitations, which cause temperature gradients inside the sample and inside each particle.

Fig. 2 shows that the decomposition of miscanthus started around 250 °C and continued up to 400 °C with peak decomposition between

310 °C and 364 °C, increasing with the heating rate. The peak decomposition rate in every case was similar to the heating rate, showing the heat transfer as the controlling step for thermal decomposition of miscanthus. On the other hand, AHR decomposition occurred in a wider temperature range (see Fig. 3), between 200 °C and 700 °C with higher peak decomposition temperatures (325 °C to 429 °C) and lower peak decomposition rates. The lower reactivity of the AHR is a result of the decomposition of most of the sugars in cellulose and hemicellulose during the acid hydrolysis process (cellulose and hemicellulose decompose at lower temperatures than lignin when heated in inert conditions [49,50]) and the formation of refractory humins.

Table 4 shows the characteristics for the pyrolysis decomposition curves of miscanthus and its AHR showed in Fig. 2 and Fig. 3 respectively; presenting also a comparison with values reported in the literature for miscanthus. The table shows that the results obtained in the present work agree with those reported in the literature at different heating rates used to calculate the decomposition curves. Peak decomposition rates were achieved at 310 °C for 2.5 °C/min, similar temperature to the average reported by Greenhalf et al. for miscanthus harvested at different seasons [51]. The results obtained at 25 °C/min agree with those reported by Mos et al. at 20 °C/min.

Table 4 also shows a comparison between the thermal decomposition characteristics of miscanthus and AHR with those reported by Yang et al. [50] and Cheng et al. [57] for the main components of biomass: cellulose, hemicellulose (using xylan as model compound) and lignin. The main decomposition temperatures reported by Cheng et al. [57] were low when compared to the data reported in the literature for miscanthus probably due to the inclusion of low heating rates during the study. The main decomposition peak for miscanthus (310 to 364 °C) was between the temperatures reported by Yang et al. for xylan and lignin, showing synergy between the fractions during the decomposition of the untreated feedstock. On the other hand, the main decomposition peak for AHR occurred at the same temperature than the reported by Yang et al. for lignin at the same heating rate indicating similar peaks for lignin and humins which are the main components of the residue.

4.3. Determination of the activation energy

The isoconversional methods described in Sections 3.1 to 3.4 were applied in steps of 10 wt.% of conversion (on a dry basis). The linearity of the isoconversional curves was checked for each conversion for the

Table 4

Comparison of TGA characteristics for miscanthus, biomass components and AHR found in literature and the present work.

Feedstock	Heating rate (°C/min)	Decomposition range (°C)	Peak degradation temperature (°C)	Max. degradation rate (wt.%/°C)	Reference
<i>Miscanthus giganteus</i>	20	Not reported	362	0.775	[6]
<i>Miscanthus giganteus</i>	2.5	Not reported	318.6	1.360	[51]
			(average)		
<i>Miscanthus sacchariflorus</i>	10	200–375	340.6	0.080	[52]
<i>Miscanthus</i>	40	280–400	315	Not reported	[53]
<i>Miscanthus sinensis</i>	10	200–500	335	~0.580	[54]
<i>Miscanthus</i>	Not reported	250–350	304	Not reported	[55]
<i>Miscanthus sinensis</i>	20	267–405	372	0.010	[56]
Cellulose	10	315–400	355	0.280	[50]
Xylan		220–315	298	0.100	
Lignin		200–900	410	0.010	
Avicel®PH-101 cellulose	1–65	Not reported	267	0.004–8.900	[57]
Xylan from Birchwood			223		
Organosolv lignin			300		
<i>Miscanthus giganteus</i>	2.5	250–410	310	1.000	This work
	5		326	0.980	
	10		337	0.990	
	17		347	0.982	
	25		364	0.944	
AHR from miscanthus	2.5	200–700	385	0.280	
	5		401	0.260	
	10		410	0.260	
	17		416	0.259	
	25		429	0.260	

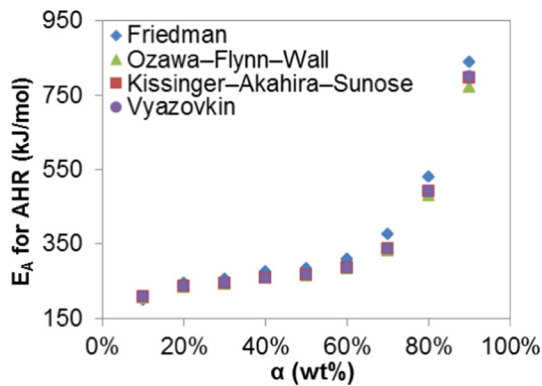


Fig. 4. Variation of the activation energy with conversion and calculation coefficients for pyrolysis of AHR from miscanthus by lineal (Friedman, Ozawa, Kissinger) and non-linear (Vyazovkin) methods.

linear approximations (Friedman, Kissinger–Akahira–Sunose, Ozawa–Flynn–Wall) by calculating the linear correlation coefficient. The minimization of the $\Omega(E_A)$ function of the Vyazovkin method also was performed for each isoconversional curve. The coefficient results and the values of E_A calculated by each isoconversional method are presented in Fig. 3 for miscanthus and in Fig. 4 for AHR.

Close similarity in the results of the activation energy values calculated by the three different integral model-free methods (Kissinger–Akahira–Sunose, Ozawa–Flynn–Wall, Vyazovkin) can be observed in Figs. 2 and 3. This result agrees with other works presented in the literature comparing kinetic parameters determined by TGA and calculated by different methods [13,18,19]. The activation energy values obtained by the Friedman method were also similar to those calculated with integral methods, as reported by Hilten et al. [47]. However, the correlation coefficients were higher for the lineal integral methods at almost every conversion value. The activation energy of both feedstocks exhibited a similar trend increasing with conversion, which indicates that the thermal decomposition is not a single reaction process. The increase with conversion was more pronounced for the AHR. The values for activation energy of the AHR were higher than the values for miscanthus in the whole conversion range. The higher values agree with the nature of the feedstock, which has already undergone chemical decomposition forming more stable components.

The highest activation energy values were obtained at 90 wt.% conversion, for which linear correlation coefficient had the lowest value and the $\Omega(E_A)$ function the highest. The variation can be attributed to the mass and heat transfer limitations observed at the highest heating rates used for the TGA measurements, which cause variations on the conversion vs. temperature data used to determine the isoconversional lines. Data obtained at conversions above 90 wt.% were ignored for the kinetic parameters calculation as the temperature integral approximations clearly did not apply for the final decomposition stage.

Table 5

Kinetic parameters determined by TGA for different feedstocks.

Feedstock		Reaction order	E_A (kJ/mol)	k_0 (s^{-1})	Reference
MG		3	113–143	$9.3(10)^8$ – $6.5(10)^{11}$	Present work
AHR–MG			200–376	$3.5(10)^{14}$ – $1.3(10)^{24}$	
Miscanthus straw	Hemicellulose	0.45–0.55	114–199	$4.4(10)^5$ – $2.4(10)^7$	[61]
	Cellulose	0.91–1.0031	86–100	$2.4(10)^7$ – $1.6(10)^{15}$	
Avicel®PH-101 cellulose		1	146–162	$4.1(10)^{11}$ – $9.1(10)^{11}$	[57]
Xylan from birchwood			156–160	$3.6(10)^{13}$ – $2.8(10)^{15}$	
Organosolv lignin			112–162	$1.4(10)^9$ – $8.3(10)^9$	
Alkali lignin		3	52	$3.4(10)^1$	[62]
Aspen wood lignin		1	61–172	$1.6(10)^{10}$	[60]
Asian lignin (straw and grass)		1.06	134	$4.1(10)^8$	[48]
Klason lignin (cassava stalk)		1.53	172	$1.5(10)^{11}$	
Klason lignin (willow)		1.53	157	$2.0(10)^{10}$	

Table 6

Values for the optimization function calculation to determine the model that fits best the experimental values of the weight loss derivative.

Feedstock	MG	AHR–MG
α at DTG maximum	57%	43%
E_A (kJ/mol)	136	260
Reaction model	Value for omega function $\Omega(E_A)$	
Reaction order	Order 0	$>10^6$
	Order 1	2630
	Order 2	2
	Order 3	0
Nucleation (Power law)	$>10^6$	$>10^6$
Nucleation (Avrami)	61,283	3033
Phase boundary	$>10^6$	$>10^6$
Diffusional	$>10^6$	$>10^6$

Fig. 4 shows the activation energy of both miscanthus and AHR exhibit a slight increase with conversion up to 70 wt.% for miscanthus and 80 wt.% for AHR. Beyond these values, the activation energy for both feedstocks increases steeply showing advanced thermal decomposition and the production of unreactive chars. Within the whole conversion range, the activation energy for pyrolysis of AHR was higher than the value for miscanthus, showing the influence of the volatiles content in the decomposition process.

The activation energy values determined for miscanthus ($E_A = 113$ – 143 kJ/mol) were similar to the values reported for the decomposition of the cellulose fraction in miscanthus by Jeguirim [58], who reported activation energies of 86–100 kJ/mol for the hemicellulose fraction and 114–199 kJ/mol for the cellulose fraction of the feedstock (see Table 5). The activation energy values determined for AHR ($E_A = 200$ – 376 kJ/mol) were considerably higher than the values reported for commercial alkali lignin (calculated using the Coats–Redfern approximation) and slightly higher than the value reported for lignin from enzymatic hydrolysis of wheat straw: 27–51 kJ/mol [59] and 107 kJ/mol [13] respectively. The values were also higher than those reported for 9 different types of lignin which were calculated by Jiang et al. using the Kissinger method [48] and those reported by Avni and Coughlin calculated for Aspen wood lignin using the differential method [60] (see Table 5). Differences between activation energy of different types of lignin and AHR can be attributed to the difference in the content of refractory humins in of the samples. The amount of humins in the sample depends on the sugars in the original feedstock and the conditions used for the separation of lignin and production of AHR.

4.4. Determination of the reaction model and the pre-exponential factor

The determination of the best reaction model was performed as described before. The value of the optimization function for each model was calculated using the activation energy determined by

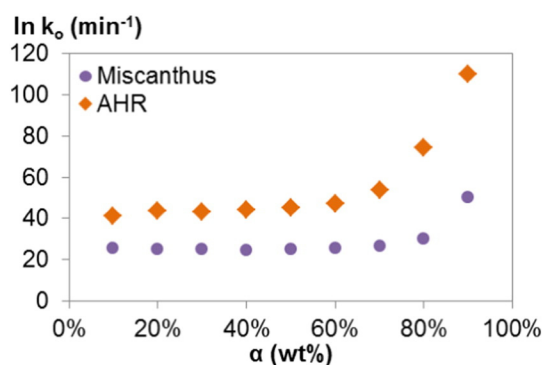


Fig. 5. Values for the pre-exponential factor k_0 (in min^{-1}) calculated using the activation energy value determined by the Vyazovkin method and the third order reaction model.

isoconversional methods. The values of the optimization function for all the reaction models considered are presented in Table 6 for all the feedstocks. The best fitting model for miscanthus and AHR was the third order reaction. The second and first order reaction closely followed the third order model as best fit for miscanthus. The third order reaction model was also determined as best fit for lignin rich acid hydrolysis residues by Huang et al. [62].

After determining the best fitting model, the pre-exponential factor was calculated at different conversion values. Since there is a compensating mathematical effect in the equations used [12,63], the pre-exponential factor also varied with the concentration (and the activation energy). The pre-exponential factor values varied from 5.6×10^{10} to $3.9 \times 10^{13} \text{ min}^{-1}$ for miscanthus and from 2.1×10^{16} to $7.7 \times 10^{25} \text{ min}^{-1}$ for AHR in the range of 10 to 90 wt.% conversion. The results for the pre-exponential factors of both feedstocks as function of conversion are presented in Figs. 5 and 6.

Fig. 6 shows modelled and experimental TGA curves for miscanthus and its AHR at the five heating rates evaluated. The results of the model-fitting on the modelled TGA curves show that the pyrolysis process is controlled by three dimensional diffusions up to the point of maximum DTG. After this point, the process is controlled by the chemical reaction following a third order model. The E_A and k_0 values were calculated at maximum DTG peak using the Vyazovkin method to build the modelled conversion curves for both parts of the process. The figure shows substantial agreement between experimental and modelled conversion curves for miscanthus, however two reaction models and values for activation energy were needed to model the decomposition process in the temperature range.

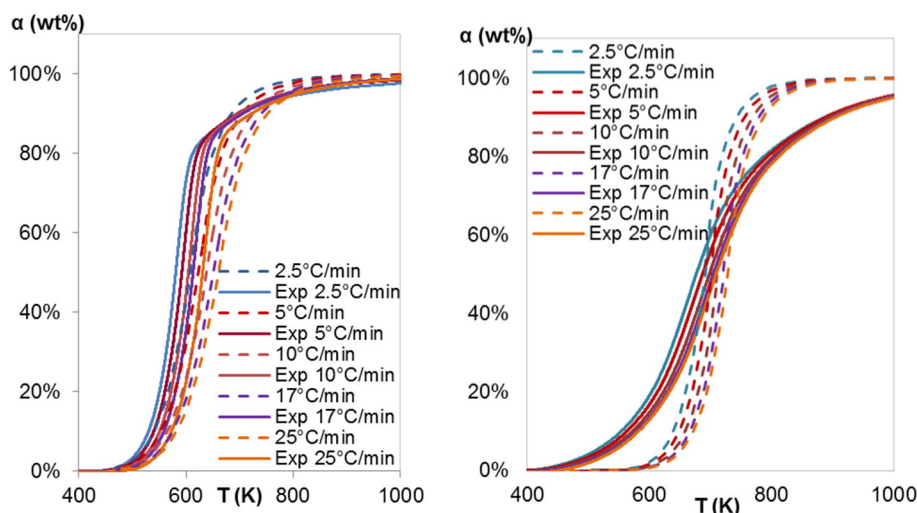


Fig. 6. Modelled (dashed) and experimental (solid) pyrolysis conversion curves as a function of temperature for miscanthus (left) and AHR (right).

Precise fitting between simulated and experimental curves of TGA pyrolysis was reported by Huang et al. for a number of agricultural residues using the KAS method. In this case, the reaction order was defined as a function of conversion instead of the activation energy, meaning the kinetic parameters were varied along the conversion range studied to build the modelled curves [59]. Accurate fits between modelled and experimental curves have been reported by Gil et al. for wood chips using the differential method, by modelling the thermal decomposition lines using the E_A calculated for each conversion value [14]. This approach gives almost perfect fitting curves but it is not a model for the whole process as different values of activation energy are used. Skreiberg et al. reported close fitting of experimental and modelled curves for pyrolysis of demolition wood, coffee residues and glossy paper using a first order isothermal approach [64], meaning the E_A value was valid only for the single heating rate at which experiments and activation energy calculations were performed.

The discrepancy between modelled and experimental lines was higher for AHR, for which the modelled curves presented a steeper increase in conversion with increasing temperature than the experimental curves. Modelled curves showed lower conversions at temperatures below $430 \text{ }^\circ\text{C}$, faster decomposition in the whole temperature range and higher final conversions than the experimental curves. Due to the low reactivity of the AHR, the decomposition of AHR is probably influenced by heat and mass transfer limitations not reflected by any of the models. The fitting between modelled and experimental TGA curves was not improved by the application of any of the other 11 models commonly used in TGA kinetics calculations and presented in Table 2. Complex models including mass and heat transfer parameters as well as chemical reaction parameters are probably required to achieve better agreement between experimental and modelled curves for the AHR. However, the kinetic parameters calculated in the present work and the model determination can be considered as a simplified base for simulation of pyrolysis applications of miscanthus and AHR.

5. Conclusions

As interest grows in chemical recovery from biomass as opposed to energy and biofuels, there will be greater quantities of processing residues arising from such processes. Utilisation of such residues for process energy and heat requirements will be essential for maximising overall process efficiency. The reactivity of acid hydrolysis residues is strongly influenced by the severity of the hydrolysis process conditions and the material tested here represents a relatively low reactivity material. As hydrolysis processes such as this develop, optimisation is required which balances the extent of hydrolysis with the potential for

recovering valuable products from the residues through holistic optimisation of the whole process. It is believed that this is the first time that the pyrolysis kinetics of acid hydrolysis residues has been systematically analysed, and thus identifies the consequences of severe hydrolysis conditions on the usefulness of residues.

The kinetic parameters activation energy, pre-exponential factor and reaction model for the pyrolysis of miscanthus and its acid hydrolysis residue were successfully calculated using thermogravimetric analysis and four different model-free calculation methods. The systematic study allowed the following conclusions to be drawn.

- The thermogravimetric curves shift to higher temperature values as the heating rate increases due to the increasing effect of heat transfer limitations.
- There is negligible difference in the kinetic parameters of pyrolysis calculated by the three integral methods (Kissinger–Akahira–Sunose, Ozawa–Flynn–Wall, Vyazovkin) and the one differential (Friedman) method. However, the integral methods gave better fitting results.
- The multiple reactions taking place as the pyrolysis decomposition advances, causes the activation energy to vary with conversion. Due to the mathematical dependence of the calculation, the pre-exponential factor also varies with conversion.
- The activation energy for AHR (268 kJ/mol) was higher than the value for miscanthus (155 kJ/mol) demonstrating the lower reactivity of the AHR.
- The decomposition of both feedstocks was best modelled by the third order reaction model.

Acknowledgements

The authors acknowledge gratefully the European Commission for financial support of the research carried out under the FP7 DIBANET project “The Production of Sustainable Diesel-Miscible-Biofuels from the Residues and Wastes of Europe and Latin America”; (Grant number 227248–2).

References

- [1] N.S. Yuzbasi, N. Selçuk, Air and oxy-fuel combustion characteristics of biomass/lignite blends in TGA–FTIR, *Fuel Process. Technol.* 92 (2011) 1101–1108, <http://dx.doi.org/10.1016/j.fuproc.2011.01.005>.
- [2] B. Girisuta, B. Danon, R. Manurung, L.P.B.M. Janssen, H.J. Heeres, Experimental and kinetic modelling studies on the acid-catalysed hydrolysis of the water hyacinth plant to levulinic acid, *Bioresour. Technol.* 99 (2008) 8367–8375, <http://dx.doi.org/10.1016/j.biortech.2008.02.045>.
- [3] B. Girisuta, K.G. Kalogiannis, K. Dussan, J.J. Leahy, M.H.B. Hayes, S.D. Stefanidis, et al., An integrated process for the production of platform chemicals and diesel miscible fuels by acid-catalyzed hydrolysis and downstream upgrading of the acid hydrolysis residues with thermal and catalytic pyrolysis, *Bioresour. Technol.* 126 (2012) 92–100, <http://dx.doi.org/10.1016/j.biortech.2012.09.013>.
- [4] T.M.C. Hoang, L. Lefferts, K. Seshan, Valorization of humin-based byproducts from biomass processing—a route to sustainable hydrogen, *ChemSusChem* (2013) <http://dx.doi.org/10.1002/cssc.201300446> (n/a–n/a).
- [5] T.M.C. Hoang, E.R.H. van Eck, W.P. Bula, J.G.E. Gardeniens, L. Lefferts, K. Seshan, Humin based by products from bioprocessing as potential carbonaceous source for synthesis gas production, *Green Chem.* (ISSN: 1463-9262) 17 (2) (2015) 959–972 (<http://doc.utwente.nl/92642/1/c4gc01324g.pdf> (accessed March 27, 2015)).
- [6] M. Mos, S.W. Banks, D.J. Nowakowski, P.R.H. Robson, A.V. Bridgwater, I.S. Donnison, Impact of *Miscanthus* × *giganteus* senescence times on fast pyrolysis bio-oil quality, *Bioresour. Technol.* 129 (2013) 335–342, <http://dx.doi.org/10.1016/j.biortech.2012.11.069>.
- [7] R. Lou, S. Wu, Products properties from fast pyrolysis of enzymatic/mild acidolysis lignin, *Appl. Energy* 88 (2011) 316–322, <http://dx.doi.org/10.1016/j.apenergy.2010.06.028>.
- [8] R.R. Keuleers, J.F. Janssens, H.O. Desseyn, Comparison of some methods for activation energy determination of thermal decomposition reactions by thermogravimetry, *Thermochim. Acta* 385 (2002) 127–142, [http://dx.doi.org/10.1016/S0040-6031\(01\)00720-1](http://dx.doi.org/10.1016/S0040-6031(01)00720-1).
- [9] A.V. Bridgwater, An introduction to fast pyrolysis of biomass for fuels and chemicals, in: A.V. Bridgwater, S. Czernik, J. Diebold, D. Meier, A. Oasmaa, C. Peacocke, et al., (Eds.), *Fast Pyrolysis Biomass A Handbook*, Vol. 1, CPL Press, Birmingham, 1999.
- [10] R.A. Naranjo, J.A. Conesa, E.F. Pedretti, O.R. Romero, Kinetic analysis: simultaneous modelling of pyrolysis and combustion processes of dichrostachys cinerea, *Biomass Bioenergy* 36 (2012) 170–175, <http://dx.doi.org/10.1016/j.biombioe.2011.10.032>.
- [11] A. Saddawi, J.M. Jones, A. Williams, M.A. Wójtowicz, Kinetics of the thermal decomposition of biomass, *Energy Fuel* 24 (2009) 1274–1282, <http://dx.doi.org/10.1021/e9909933k>.
- [12] J.E. White, W.J. Catallo, B.L. Legendre, Biomass pyrolysis kinetics: a comparative critical review with relevant agricultural residue case studies, *J. Anal. Appl. Pyrolysis* 91 (2011) 1–33, <http://dx.doi.org/10.1016/j.jaap.2011.01.004>.
- [13] Q. Yang, S. Wu, Thermogravimetric characteristics of wheat straw lignin, *Cellul. Chem. Technol.* 43 (2009) 133–139 (<http://www.cellulosechemtechnol.ro/pdf/CCT4-6-2009/133-139.pdf>).
- [14] M.V. Gil, D. Casal, C. Pevida, J.J. Pis, F. Rubiera, A.V. Bridgwater, Thermal behaviour and kinetics of coal/biomass blends during co-combustion, *Bioresour. Technol.* 8 (2004) 21–49, <http://dx.doi.org/10.1016/j.biortech.2010.02.008>.
- [15] J.-L. Dirion, C. Reverte, M. Cabassud, Kinetic parameter estimation from TGA: Optimal design of TGA experiments, n.d.
- [16] C. Di Blasi, Combustion and gasification rates of lignocellulosic chars, *Prog. Energy Combust. Sci.* 35 (2009) 121–140, <http://dx.doi.org/10.1016/j.peccs.2008.08.001>.
- [17] F. Carrasco, The evaluation of kinetic parameters from thermogravimetric data: comparison between established methods and the general analytical equation, *Thermochim. Acta* 213 (1993) 115–134, [http://dx.doi.org/10.1016/0040-6031\(93\)80010-8](http://dx.doi.org/10.1016/0040-6031(93)80010-8).
- [18] A. Ounas, A. Aboulkas, K. El harfi, A. Bacaoui, A. Yaacoubi, Pyrolysis of olive residue and sugar cane bagasse: non-isothermal thermogravimetric kinetic analysis, *Bioresour. Technol.* 102 (2011) 11234–11238, <http://dx.doi.org/10.1016/j.biortech.2011.09.010>.
- [19] T. Damartzis, D. Vamvuka, S. Sfakiotakis, A. Zabaniotou, Thermal degradation studies and kinetic modeling of cardoon (*Cynara cardunculus*) pyrolysis using thermogravimetric analysis (TGA), *Bioresour. Technol.* 102 (2011) 6230–6238, <http://dx.doi.org/10.1016/j.biortech.2011.02.060>.
- [20] ASTM, Standard Test Method for Compositional Analysis by Thermogravimetry, 2003, <http://dx.doi.org/10.1520/E1131-03>.
- [21] ASTM, Standard Test Method for Ash in Biomass, 2001, <http://dx.doi.org/10.1520/E1755-01R07>.
- [22] S.A. Channiwala, P.P. Parikh, A unified correlation for estimating HHV of solid, liquid and gaseous fuels, *Fuel* 81 (2002) 1051–1063, [http://dx.doi.org/10.1016/S0016-2361\(01\)00131-4](http://dx.doi.org/10.1016/S0016-2361(01)00131-4).
- [23] T. Ona, T. Sonoda, M. Shibata, K. Fukuzawa, Small-scale method to determine the content of wood components from multiple eucalypt samples, *TAPPI J.* 78 (1995).
- [24] ASTM E1641-07, Standard Test Method for Decomposition Kinetics by Thermogravimetry, ASTM International, West Conshohocken, PA 2007, pp. 1–6, <http://dx.doi.org/10.1520/E1641-07>. www.astm.org.
- [25] A. Khawam, Application of Solid-state Kinetics to Desolvation Reactions, University of Iowa, 2007.
- [26] L. Gašparovič, Z. Koreňová, Ľ. Jelemenský, Kinetic study of wood chips decomposition by TGA, *Chem. Pap.* 64 (2010) 174–181, <http://dx.doi.org/10.2478/s11696-009-0109-4>.
- [27] N. Sbirrazzuoli, Is the Friedman method applicable to transformations with temperature dependent reaction heat? *Macromol. Chem. Phys.* 208 (2007) 1592–1597, <http://dx.doi.org/10.1002/macp.200700100>.
- [28] B. Jankovi, Thermal stability investigation and the kinetic study of Folsn@ degradation process under nonisothermal conditions, *AAPS PharmSciTech* 11 (2010) 103–112, <http://dx.doi.org/10.1208/s12249-009-9363-6>.
- [29] N. Sbirrazzuoli, L. Vincent, A. Mija, N. Guigo, Integral, differential and advanced isoconversional methods: complex mechanisms and isothermal predicted conversion–time curves, *Chemom. Intell. Lab. Syst.* 96 (2009) 219–226, <http://dx.doi.org/10.1016/j.chemolab.2009.02.002>.
- [30] L. Pérez-Maqueda, J. Criado, The Accuracy of Senum and Yang's approximations to the Arrhenius integral, *J. Therm. Anal. Calorim.* 60 (2000) 909–915, <http://dx.doi.org/10.1023/a:1010115926340>.
- [31] S. Vyazovkin, D. Dollimore, Linear and nonlinear procedures in isoconversional computations of the activation energy of nonisothermal reactions in solids, *J. Chem. Inf. Comput. Sci.* 36 (1996) 42–45, <http://dx.doi.org/10.1021/ci950062m>.
- [32] M. Amutio, G. Lopez, J. Alvarez, R. Moreira, G. Duarte, J. Nunes, et al., Pyrolysis kinetics of forestry residues from the Portuguese Central Inland Region, *Chem. Eng. Res. Des.* 91 (2013) 2682–2690, <http://dx.doi.org/10.1016/j.cherd.2013.05.031>.
- [33] N. Brosse, A. Dufour, X. Meng, Q. Sun, A. Ragauskas, Miscanthus: a fast-growing crop for biofuels and chemicals production, *Biofuels, Bioprod. Biorefining.* 6 (2012) 580–598, <http://dx.doi.org/10.1002/bbb.1353>.
- [34] P. McKendry, Energy production from biomass (part 1): overview of biomass, *Bioresour. Technol.* 83 (2002) 37–46, [http://dx.doi.org/10.1016/S0960-8524\(01\)00118-3](http://dx.doi.org/10.1016/S0960-8524(01)00118-3).
- [35] K.O. Davidsson, J.G. Korsgren, J.B.C. Pettersson, U. Jäglid, The effects of fuel washing techniques on alkali release from biomass, *Fuel* 81 (2002) 137–142, [http://dx.doi.org/10.1016/S0016-2361\(01\)00132-6](http://dx.doi.org/10.1016/S0016-2361(01)00132-6).
- [36] T. Hsu, Q. Nguyen, Analysis of solids resulted from dilute-acid pretreatment of lignocellulosic biomass, *Biotechnol. Tech.* 9 (1995) 25–28, <http://dx.doi.org/10.1007/BF00152994>.
- [37] Z.A. Mayer, A. Apfelbacher, A. Hornung, Effect of sample preparation on the thermal degradation of metal-added biomass, *J. Anal. Appl. Pyrolysis* 94 (2012) 170–176, <http://dx.doi.org/10.1016/j.jaap.2011.12.008>.
- [38] D. Park, Y.-S. Yun, J.M. Park, Studies on hexavalent chromium biosorption by chemically-treated biomass of *Ecklonia* sp, *Chemosphere* 60 (2005) 1356–1364, <http://dx.doi.org/10.1016/j.chemosphere.2005.02.020>.
- [39] D. Vamvuka, S. Troulino, E. Kastanaki, The effect of mineral matter on the physical and chemical activation of low rank coal and biomass materials, *Fuel* 85 (2006) 1763–1771, <http://dx.doi.org/10.1016/j.fuel.2006.03.005>.

- [40] S. Banks, Ash Control Methods to Limit Biomass Inorganic Content and Its Effect on Fast Pyrolysis Bio-oil Stability, Aston University, 2014.
- [41] S.S. Idris, N.A. Rahman, K. Ismail, Combustion characteristics of Malaysian oil palm biomass, sub-bituminous coal and their respective blends via thermogravimetric analysis (TGA), *Bioresour. Technol.* 123 (2012) 581–591, <http://dx.doi.org/10.1016/j.biortech.2012.07.065>.
- [42] P. Pimenidou, V. Dupont, Characterisation of palm empty fruit bunch (PEFB) and pinewood bio-oils and kinetics of their thermal degradation, *Bioresour. Technol.* 109 (2012) 198–205, <http://dx.doi.org/10.1016/j.biortech.2012.01.020>.
- [43] D.K. Seo, S.S. Park, J. Hwang, T.-U. Yu, Study of the pyrolysis of biomass using thermo-gravimetric analysis (TGA) and concentration measurements of the evolved species, *J. Anal. Appl. Pyrolysis* 89 (2010) 66–73, <http://dx.doi.org/10.1016/j.jaap.2010.05.008>.
- [44] S.S. Idris, N.A. Rahman, K. Ismail, A.B. Alias, Z.A. Rashid, M.J. Aris, Investigation on thermochemical behaviour of low rank Malaysian coal, oil palm biomass and their blends during pyrolysis via thermogravimetric analysis (TGA), *Bioresour. Technol.* 101 (2010) 4584–4592, <http://dx.doi.org/10.1016/j.biortech.2010.01.059>.
- [45] O.P. Korobeinichev, A.A. Paletsky, M.B. Gonchikzhapov, I.K. Shundrina, H. Chen, N. Liu, Combustion chemistry and decomposition kinetics of forest fuels, *Procedia Eng.* 62 (2013) 182–193, <http://dx.doi.org/10.1016/j.proeng.2013.08.054>.
- [46] D. Chen, Y. Zheng, X. Zhu, In-depth investigation on the pyrolysis kinetics of raw biomass. Part I: kinetic analysis for the drying and devolatilization stages, *Bioresour. Technol.* 131 (2013) 40–46, <http://dx.doi.org/10.1016/j.biortech.2012.12.136>.
- [47] R. Hilten, J.P. Vandenbrink, A.H. Paterson, F.A. Feltus, K.C. Das, Linking isoconversional pyrolysis kinetics to compositional characteristics for multiple *Sorghum bicolor* genotypes, *Thermochim. Acta* 577 (2014) 46–52, <http://dx.doi.org/10.1016/j.tca.2013.12.012>.
- [48] G. Jiang, D.J. Nowakowski, A.V. Bridgwater, A systematic study of the kinetics of lignin pyrolysis, *Thermochim. Acta* 498 (2010) 61–66, <http://dx.doi.org/10.1016/j.tca.2009.10.003>.
- [49] L. Burhenne, J. Messmer, T. Aicher, M.-P. Laborie, The effect of the biomass components lignin, cellulose and hemicellulose on TGA and fixed bed pyrolysis, *J. Anal. Appl. Pyrolysis* 101 (2013) 177–184, <http://dx.doi.org/10.1016/j.jaap.2013.01.012>.
- [50] H. Yang, R. Yan, H. Chen, D.H. Lee, C. Zheng, Characteristics of hemicellulose, cellulose and lignin pyrolysis, *Fuel* 86 (2007) 1781–1788, <http://dx.doi.org/10.1016/j.fuel.2006.12.013>.
- [51] C.E. Greenhalf, D.J. Nowakowski, N. Yates, I. Shield, A.V. Bridgwater, The influence of harvest and storage on the properties of and fast pyrolysis products from *Miscanthus × giganteus*, *Biomass Bioenergy* 56 (2013) 247–259, <http://dx.doi.org/10.1016/j.biombioe.2013.05.007>.
- [52] J.-Y. Kim, S. Oh, H. Hwang, Y.-H. Moon, J.W. Choi, Assessment of miscanthus biomass (*Miscanthus sacchariflorus*) for conversion and utilization of bio-oil by fluidized bed type fast pyrolysis, *Energy* 76 (2014) 284–291, <http://dx.doi.org/10.1016/j.energy.2014.08.010>.
- [53] K. Jayaraman, I. Gökalp, Pyrolysis, combustion and gasification characteristics of miscanthus and sewage sludge, *Energy Convers. Manag.* 89 (2015) 83–91, <http://dx.doi.org/10.1016/j.enconman.2014.09.058>.
- [54] J.P. Bok, H.S. Choi, J.W. Choi, Y.S. Choi, Fast pyrolysis of *Miscanthus sinensis* in fluidized bed reactors: characteristics of product yields and biocrude oil quality, *Energy* 60 (2013) 44–52, <http://dx.doi.org/10.1016/j.energy.2013.08.024>.
- [55] E. Butler, G. Devlin, D. Meier, K. McDonnell, Characterisation of spruce, salix, miscanthus and wheat straw for pyrolysis applications, *Bioresour. Technol.* 131 (2013) 202–209, <http://dx.doi.org/10.1016/j.biortech.2012.12.013>.
- [56] E. Mészáros, G. Várhegyi, E. Jakab, B. Marosvölgyi, Thermogravimetric and reaction kinetic analysis of biomass samples from an energy plantation, *Energy Fuel* 18 (2004) 497–507, <http://dx.doi.org/10.1021/ef034030>.
- [57] K. Cheng, W.T. Winter, A.J. Stipanovic, A modulated-TGA approach to the kinetics of lignocellulosic biomass pyrolysis/combustion, *Polym. Degrad. Stab.* 97 (2012) 1606–1615, <http://dx.doi.org/10.1016/j.polymdegradstab.2012.06.027>.
- [58] M. Jeguirim, S. Dorge, A. Loth, G. Trouvé, Devolatilization kinetics of miscanthus straw from thermogravimetric analysis, *Int. J. Green Energy* 7 (2010) 164–173, <http://dx.doi.org/10.1080/15435071003673641>.
- [59] Y.F. Huang, W.H. Kuan, P.T. Chiueh, S.L. Lo, A sequential method to analyze the kinetics of biomass pyrolysis, *Bioresour. Technol.* 102 (2011) 9241–9246, <http://dx.doi.org/10.1016/j.biortech.2011.07.015>.
- [60] E. Avni, R.W. Coughlin, Kinetic analysis of lignin pyrolysis using non-isothermal TGA data, *Thermochim. Acta* 90 (1985) 157–167, [http://dx.doi.org/10.1016/0040-6031\(85\)87093-3](http://dx.doi.org/10.1016/0040-6031(85)87093-3).
- [61] M. Jeguirim, S. Dorge, G. Trouvé, Thermogravimetric analysis and emission characteristics of two energy crops in air atmosphere: *Arundo donax* and *Miscanthus giganteus*, *Bioresour. Technol.* 101 (2010) 788–793, <http://dx.doi.org/10.1016/j.biortech.2009.05.063>.
- [62] Y. Huang, Z. Wei, X. Yin, C. Wu, Pyrolytic characteristics of biomass acid hydrolysis residue rich in lignin, *Bioresour. Technol.* 103 (2012) 470–476, <http://dx.doi.org/10.1016/j.biortech.2011.10.027>.
- [63] P. Budrugaec, E. Segal, Some methodological problems concerning nonisothermal kinetic analysis of heterogeneous solid–gas reactions, *Int. J. Chem. Kinet.* 33 (2001) 564–573, <http://dx.doi.org/10.1002/kin.1052>.
- [64] A. Skreiberg, Ø. Skreiberg, J. Sandquist, L. Sørum, TGA and macro-TGA characterisation of biomass fuels and fuel mixtures, *Fuel* 90 (2011) 2182–2197, <http://dx.doi.org/10.1016/j.fuel.2011.02.012>.